

# Interdisciplinary Design Study of a High-rise Integrated Roof Wind Energy System

R.W.A. Dekker<sup>1,a</sup>, R.M. Ferraro<sup>1</sup>, A.B. Suma<sup>1</sup>, and S.P.G. Moonen<sup>1</sup>

<sup>1</sup>Eindhoven University of Technology, Department of Built Environment, 5612AZ Eindhoven, the Netherlands

**Abstract.** Today's market in micro-wind turbines is in constant development introducing more efficient solutions for the future. Besides the private use of tower supported turbines, opportunities to integrate wind turbines in the built environment arise. The Integrated Roof Wind Energy System (IRWES) presented in this work is a modular roof structure integrated on top of existing or new buildings. IRWES is build up by an axial array of skewed shaped funnels used for both wind inlet and outlet. This inventive use of shape and geometry leads to a converging air capturing inlet to create high wind mass flow and velocity toward a Vertical Axis Wind Turbine (VAWT) in the center-top of the roof unit for the generation of a relatively high amount of energy. The scope of this research aims to make an optimized structural design of IRWES to be placed on top of the Vertigo building in Eindhoven; analysis of the structural performance; and impact to the existing structure by means of Finite Element Modeling (FEM). Results show that the obvious impact of wind pressure to the structural design is easily supported in different configurations of fairly simple lightweight structures. In particular, the weight addition to existing buildings remains minimal.

## 1 Introduction

Depredation of fossil fuels, global increasing energy costs and demand force today's society to change the energy need and generation to ensure the quality of future life and our essential ecosystems [1-3] [ENREF 2](#) [ENREF 3](#). To address this current and future need, more effective solutions for harvesting renewable energy sources on the short term are needed.

Governments, scientist and communities are looking for feasible solutions to the aforementioned problem. The EU Members adopted a binding target of 20% energy from renewable sources in final energy consumption by 2020 [4]. Compared to other energy sources, onshore wind seems to be the future largest contributor of renewable energy technologies [5]. Key factors of its advantage are that it's largely available on almost any locations, drastically reduces carbon costs, suffers from zero geo-political risk associated with supply and infrastructure constraints, as well as energy dependence [6].

Today's market in micro-wind turbines is in constant development introducing more efficient turbines for the future. Besides the private use of tower supported turbines, the opportunity to integrate wind turbines in the built environment arises [7], introducing the renewable wind energy

---

<sup>a</sup> e-mail : r.w.a.dekker@student.tue.nl

market to all residential home owners. However, today's micro-wind turbines still have low power production due to turbulent flows around the buildings, reduced wind speed in urban areas, and limited dimensions of blades [7]. Furthermore the integration of these energy systems has a substantial impact on the architecture of a structure and of the urban area as a whole [8].

The subject of this study deals with the structural design of an Integrated Roof Wind Energy System (IRWES) on an existing high-rise building which by means of a combination of external louvers and internal funnels accelerates and directs the wind flow towards an internal Vertical Axis Wind Turbines (VAWT). The system, thanks to the flow acceleration, has the potential to harvest more energy than any other comparable micro-system and to work also when the wind speed in that area is low ( $<3.6$  m/s). The objectives of this study are: 1) assess the structural performance of the IRWES implemented on a specific location; 2) examine the structural interaction of the top-up wind energy system unit with the existing building and structure, 3) develop a Finite Element Model for a load and geometrical configuration parametric study, and 4) compared results with maximum allowable stresses and deflections for different configurations and loads.

## 2 Description of the system

The concept of the Integrated Roof Wind Energy System designed by Suma in 2009 [9] is illustrated in Fig. 1. The system consists of a series of louvers on each side to guide the facade interacting wind flow inside the roof, a curved internal dome with underlying supporting structure, four internal walls dividing the funnels, and a VAWT in the centre, all enclosed by a roof top [10].

The incoming wind flow passes through a number of radial distributed inlet guide ducts, and is accelerated by their skewed shape to strike the VAWT located at the internal top of the roof. The configuration of the modular structure enables electricity generation from wind coming from any direction. The lower part of the roof has dual-purpose openings which serve as the inlets to capture incoming air flow and outlets for the outgoing air flow when wind comes from opposite direction.

At the windward facade, the incoming air flow partially includes the flow interacting with the facade of the lower regions (Fig. 1). The addition of louvers enhances the wind capturing of the effective area resulting in an increase of the total mass flow rate. Thereby the addition of louvers improves the guidance of the wind flow inside IRWES towards the VAWT, decreasing the turbulent flow in the lower part of the channel [11]. On the leeward side, a low pressure vertical base flow is formed behind the wall and beneath the roof shape. The leeward region has relative lower pressure and creates a suction effect which facilitates the exit of the flow through the outlets.

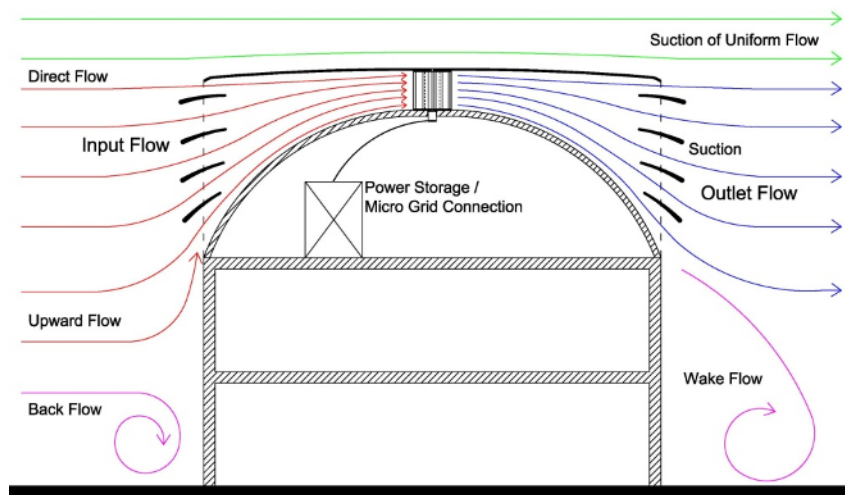


**Fig. 1.** Cross-section of flat-shaped roof with idealized incoming flow.

### 3 Case study

Aim of the integration of the wind energy system into the roof structures is to generate energy at the location where it is needed and provide an increase in the power production of micro-turbines employed in the built environment. The application of IRWES on high-rise buildings allows using the natural higher wind speed of the higher altitudes and facilitates the user's perspective.

The case study comprises the integration of IRWES on top of the Vertigo building, located in Eindhoven, at the Eindhoven University of Technology (TU/e) campus, see Fig. 2. This high-rise structure is selected based on its urban location with parkland surroundings, rectangular capacity and the benefits associated with the relationship between the research team and University.

Vertigo consists of a low-rise and high-rise part, structurally dilated from each other. Application of IRWES on the elevator shaft will only affect the high-rise section (Fig. 2 and 3). The buildings structure comprises 14 concrete portal frames placed symmetrically on the west and east wing, two concrete cores, located at the south and north ends of the high-rise part, and two concrete elevator shaft walls situated at the outer south end. The concrete material is of minimum quality C20/25 [12].



Fig. 2. IRWES on elevator shaft, Vertigo, TU/e

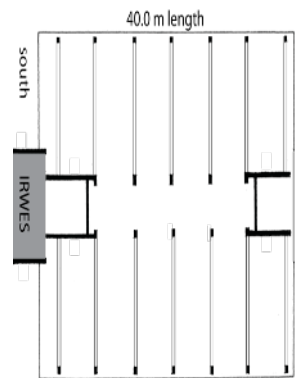


Fig. 3. Concrete structure of high-rise part Vertigo

The local prevailing average annual wind direction is South-West with a mean velocity of 3.8 m/s at a height of 10 m [13]. Integration of a wind energy system is preferred at the highest point of the building with an optimal configuration harvesting energy from the governing wind direction. With the north south orientation of Vertigo and the increased height of the elevator shaft at the south end, application of the wind energy system on top of the elevator shaft is preferred (Fig. 2 and 3).

The application of IRWES introduces additional loads to the existing bearing structure of the building. The static load increases because of its dead loads (DL). Likewise, the horizontal wind forces will increase by the enlargement of the facade area, whereby the wind flowing through the system complicates the prediction of the magnitude of these forces. The wind pressure exerts lift to IRWES' rooftop. The channel walls are laterally loaded by pressure and suction from two sides, both affecting the structural design of the system. Dynamic loads are expected, resulting from wind flow pressure, centrifugal forces associated with the VAWT, and impact forces accompanied by every turbine start-up launch. Previously described forces are carried by the existing structure, potentially with additional measures like reinforcement at the supports, enlargement of supporting walls, columns or additional columns to increase the bearing capacity.

The effect caused by addition of this system to the structural stability is of even larger importance compared to the structural strength. The module needs to provide its own stability resulting in a framework underneath the channels composition. Including stability measures within the module simplifies the application of IRWES to existing buildings. However, damping measures remain requisite to prevent vibrations entering the supporting structure. Thereby the connections need to be designed adequate to transfer the lateral loading towards the existing bearing structure. To determine

and optimise the structural loads and design of IRWES, the software Scia Engineer 2011.1 [14] is used; resulting a 3D Finite Element Method (FEM) simulation.

### 3.1 Geometry

The concept of IRWES within a roof structure was initially based on an axial symmetrical floor plan and later transformed to a squared floor plan, still containing four axes of symmetry and peer configurations of all ducts. However, integration of the energy system into a building requires smooth transition of the facades to the internal dome. Application of IRWES on Vertigo requires adaptation towards a trapezoid floor plan, reducing the axes of symmetry to two, leading to two feasible configurations of internal walls (Fig. 4). Because of the possible influence of the wind direction with respect to the internal funnels, both configurations need to be considered as options for the structural design. The optimal configuration will be selected after further analysis by means of Computation of Fluid Dynamics (CFD) [11], and testing on a full scale prototype with dimensions  $L \times B \times H$  (m) = 4 x 4 x 6.

The three dimensional model is trapezoidal shaped in plan with dimensions  $L \times B \times H$  (m) = 12.20 x 5.45 x 2.90. Fig. 4c describes the roof structure; the solid lines represent the primary beams and the dashed lines the secondary beams. This structure is enclosed by plate elements (Fig. 4b). The top roof structure is supported by columns placed on the internal dome making use of plate elements to enclose the dome (Fig. 4d). This shape is supported by a framework providing the necessary stability for the complete wind energy system, as illustrated in Fig. 4e.

The upper structure consists of portal frames; build up of columns from the internal wall on the top connected with a fixed-moment connection to the primary beam, resulting in three degrees of freedom. The span of the primary beams varies from a maximum of 4.15m in configuration A to a maximum of 3.11m in configuration B. The small span realises a reduction in structural height of the roof structure, while the air flow is minimally obstructed. Thereby, the maximum span of the louvers under the given circumstances, concerning wind loading and structural design capacity of the louvers, is not exceeded.

The secondary beams are hinged to the primary beams, providing stiffness to the roof structure acting as one plane, supporting the plate, and transferring the acting loads. The columns supporting the internal walls are placed on top of the stability framework and connected with fixed-moment connections, to enable the translation of deformations from one column to the other, while rotations are prevented. The bases of the lower columns are pinned reducing the degrees of freedom to three in rotation. Maximum lengths of previously described elements are summarised in Table 1.

**Table 1.** Maximum lengths of the elements in IRWES.

Configuration	Span [m]				
	Primary beam	Secondary Beam	Exterior/wall column	Dome column	Dome primary beam
A	4.152	2.076	2.383	1.554	4.900
B	2.940	3.114	2.383	1.554	5.188

The model specifics make use of similar nodes for the beam-ends, columns and plate elements. The node position indicates the centrally located axis of the used beam or column, while the position of the sheeting covering the beams is realised by addition of an eccentricity.

Due to required curved plate elements, situated on the west and east side of the model, had to be divided in triangular elements, as shown in the element configurations of Fig. 4b and Fig. 4d.

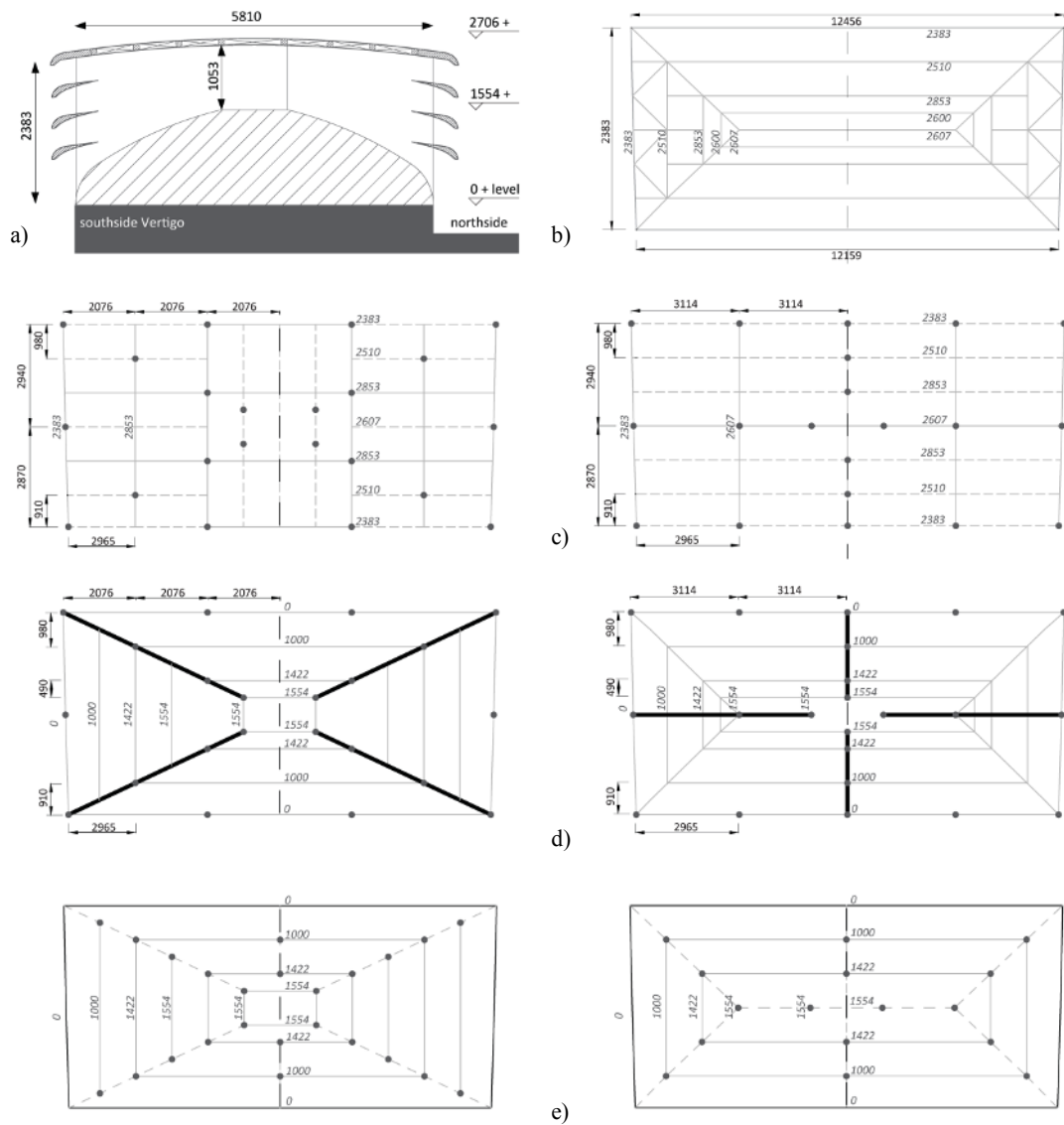


**Fig. 4.** Geometry generated in Scia Engineer [mm]: a) section; b) roof plate elements; c) roof beam structure (configuration A left, and B right); d) internal wall configuration and floor plates; e) internal dome structure.

### 3.2 Structural Analysis

Structural analysis is based on the use of aluminium for roof structure, plate elements and internal wall columns, while the dome supporting structure is made of steel. The application of both steel and aluminium requires additional attention to the connections, due to the galvanic corrosion caused by the cathodic reaction of aluminium in contact with steel. The application of IRWES on buildings requires a safety guarantee in terms of bearing capacity of the existing supporting structure and structural capacity of the system itself. Of similar importance is the need for a low maintenance system and the potential to form the material in curved aerodynamic shapes for both louvers and roof edges. The material choice based on these characteristics is easily drawn towards aluminium based on degradation, weight, maintenance and moldability. However, possible fatigue issue and costs associated drive the material selection towards a combination of aluminium and steel. Aluminium

alloy 6082-T6 [12], given its tensile strength, better general corrosion resistance through compact film of aluminium oxide, and similar extrudability and anodizing response is used for sheeting, columns and beams. The steel used for the inner dome structure is S235 [12]. The structure is analysed on strength and deformations based on the governing Eurocode [12], resulting in four different combinations in the Ultimate Limit State (ULS) to calculate the structural strength and three combinations in the Serviceability Limit State (SLS) for the deformation. All analysed Load Combinations (LC) are described in Table 2.

**Table 2.** Load combinations specifics

Load Combination (LC)	Typology	Load factor permanent load	Load factor variable load	Variable load
I	ULS	1.35	0	-
II	ULS	1.2	1.5	snow
III	ULS	0.9	1.5	wind west
IV	ULS	0.9	1.5	wind south
V	SLS	1.0	1.0	snow
VI	SLS	1.0	1.0	wind west
VII	SLS	1.0	1.0	wind south

## 4 Result and discussion

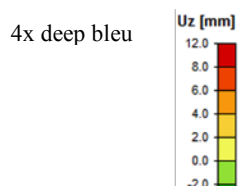
Structural analysis leads to a minimum required IPE 80 for both primary and secondary beams of the roof structure, sheeting elements of 2 mm thickness, and hollow circular shaped columns with cross-section  $d \times t = 57 \times 5$  mm. The columns of the steel structure need to be stabilised by steel x-bracings of minimal 8 mm diameter. LC II is governing for strength regarding positive normal forces in columns and shear forces in beams, while LC IV shows slightly larger negative results.

Deformation of the roof structure in downward direction is governed by snow loading and south wind in upward direction. Fig. 5 illustrates the deflections schemes of the roof structure for each internal wall configuration in the different LC's. The largest positive deflections are indicated by red with progress towards the largest negative deflections in deep blue. Lateral deflection of the columns is noticeable, partially caused by the additional lateral loading from wind on the internal walls. The south exterior columns of 2.38 m length show largest displacements in y-direction. Table 3 summarises governing stresses and deflection for each element.

**Table 3.** Governing stresses and deformations of steel and aluminium elements.

Member	Configuration A			Configuration B		
	Normal stress [MPa]	Shear stress [MPa]	Deformation [mm]	Normal stress [MPa]	Shear stress [MPa]	Deformation [mm]
Beam roof	-39.5 / +26.3	6.5	-12.7 / 7.7	-125.7 / +89.2	16.9	-14.0 / +8.0
Column exterior/wall	-103.2 / +100.2	10.5	1.1	-56.9 / +60.8	2.4	3.6
Beam dome	-8.8 / +8.2	1.6	-3.5	-49.4 / +47.7	14.0	-8.8
Column dome	-30.2 / +27.9	2.8	0.4	-17.5 / +17.2	0.4	0.2
Limit	-340 / +310*0.44	210	16 / 19.6	-235 / +235*0.44	136.3	4.8 / 3.1
	Aluminium		Beam Al/St	Steel		Col. Al/St

Maximum allowable deflection of the steel beam with largest span 19.6 mm, compared to 16 mm for the aluminium members. Tallest aluminium columns have allowable displacement of 4.8 mm, while the smaller steel columns have 3.1 mm without additional measures. Maximum normal stress in compression of steel and aluminium sections is based on buckling shape and slenderness.



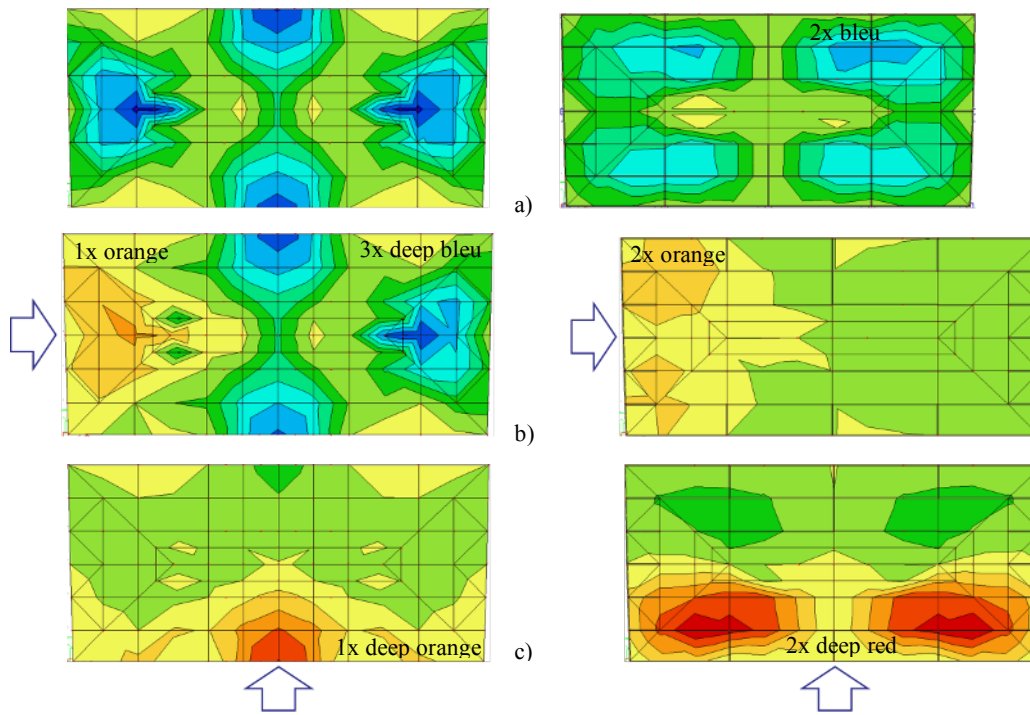


**Fig. 6.** Deformation of roof structure (configuration A = left, and B = right) for: a) snow loads LCV; b) west wind LCVI; c) south wind LCVII.

Deflections of the roof structure in both configurations are all within maximum allowable limits of 16 mm (Table 4). Snow loads result in largest downwards deflections, including four peaks in configuration A. Downward suction by west wind in configuration A is of great influence while B experiences far less influence. Concentrated uplift due to south wind in configuration A is retained better compared to B. South wind results in larger uplift compared to west wind.

The dead load of the structure in configuration A is 2668 kg, of which 322 kg comes from the aluminium supporting structure and 1146 kg is subscribed to the steel structure. The structural weight of configuration B sums to 2564 kg, with 306 kg for the aluminium parts and 1058 kg for the steel structure. The turbine is estimated to contribute approximately 100 kg to the total.

**Table 4.** deflection in

Configuration	Deflection range [mm]		
	Snow	Wind west	Wind south
A	+2.0 to -15.0	+6.0 to -12.0	+8.0 to -2.0
B	+2.0 to -10.0	+4.0 to 0.0	+12.0 to -4.0

## 5 CONCLUSION

The structural strength response in Configuration A approaches the more ideal scenario. Loads are better distributed, where vertical forces are more efficiently lead to the columns and horizontal forces to the beams. Configuration B shows that vertical and horizontal force distribution leads to more requirements in terms of moment stiffness in the nodes. Anticipating on expected vibrations and fatigue, a most efficient load distribution is required, especially in connections. However, all stresses for both configurations are within Eurocode limits.

Deformations of both configurations are within range. Striking is the difference in response to the wind load from both south and west. Structural performance of configuration A is better in LCVI

(DL and wind from west), while configuration B gives better results in LCV (DL and snow) and LCVII (DL and wind from south). The choice of material has a larger effect than the choice of configuration in terms of total weight of the structure. The aluminum structure only takes 12% into account of the weight without sheeting, while steel parts cover 43%.

## 6 Further studies

Continuing work includes experimental data measurements in a full scale model of dimensions: L x B x H (m) = 4 x 4 x 6. Vibration impact on the supporting structure will be investigated. Fatigue loading will be regarded in more detail and compared with fatigue loads on aluminium parts of comparable structures. Finally, the configuration of connections and constructability will be regarded into detail, with special attention to the steel-aluminium connections.

## 7 Acknowledges

The authors would like to acknowledge the Europe Commission and Dutch government subsidies agency STW for their financial support in the form of EP7 – Marie Curie Fellowship and STW Valorisation Grant Phase I, respectively. The financial support provided by Stiftung Mercator to attend the European Energy Conference 2012 in Maastricht is also gratefully acknowledged.

## References

1. J.P. Holdren (1991) "Population and the Energy Problem," Population and Environment: a Journal of Interdisciplinary Studies, Vol. **12**- 3, pp. 231-255
2. A. Zervos, and C. Kjaer (2009) "Pure Power," A Report by the European Wind Energy Association
3. M.A. Brown, and E. Logan (2008) "The Residential Energy and Carbon Footprints of the 100 largest U.S. Metropolitan Areas," Working Paper # 39, Georgia Institute of Technology
4. Commission of the European Community (2008) "20 20 by 2020 Europe's Climate Change Opportunity," Communication from the commission of the European parliament, The Council, the European economic and social committee and the committee of the regions
5. Europe and Renewable Energy Council (2008) "The EREC Renewable Energy Technology Roadmap 20% by 2020"
6. E. Sesto, and C. Casale (1998) "Exploitation of Wind as an Energy Source to Meet the World's Electricity Demand," Wind Engineering and Industrial Aerodynamics, Vol. **74-76**, pp. 375-287
7. D. Ayhan, and Š. Sađlam (2011) "Renewable and Sustainable Energy Reviews," A Technical Review of Building-Mounted Wind Power Systems and a Simple Stimulation Model [in-press]
8. J. Knight (2004) "Urban wind power: breezing into town," Nature, Vol. **430**, pp. 12-13
9. A.B. Suma (2010) "Wind energy system," U.S. Pat. 20100247302, University of Miami
10. A.B. Suma, R.M. Ferraro, B. Dano, and S.P.G. Moonen (2012) "Integrated Roof Wind Energy System," 2nd European Energy Conference, Maastricht, the Netherlands
11. R.M. Ferrarro, A.A. Khayrullina, A.B. Suma, and S.P.G. Moonen (2012) "Aerodynamic Study of an Integrated Roof Wind Energy System by means of Computational Fluid Dynamics Simulations," Europe's Premier Wind Energy Event, Copenhagen, Denmark
12. Technische Commissie CEN/TC 250 "Structural Eurocodes", NEN-EN 1990, 1991-1, 1992-1, 1993-1, and 1999-1 inclusief Nationale Bijlage (NL); Eurocode 0, 1, 2, 3, and 9
13. Koninklijk Nederlands Meteorologisch Instituut (2012) "Jaaroverzicht van het Weer in Nederland – 2011," KNMI, Ministerie van Verkeer en Waterstaat
14. Scia Group (2011) "Reference Guide Scia Engineer 2011"